



ON THE EIGENCHARACTERISTICS OF LONGITUDINALLY  
VIBRATING RODS WITH A CROSS-SECTION DISCONTINUITY

Ö. TURHAN

Faculty of Mechanical Engineering, Istanbul Technical University, 80191 Gümüüşsuyu, Istanbul, Turkey

(Received 16 November 2000, and in final form 5 March 2001)

1. INTRODUCTION

The eigenanalysis problem of rods with a cross-section discontinuity is a common subject of interest, also treated in textbooks [e.g., references [1, 2]]. The problem has conjugates in the area of torsional vibrations of bars, sound propagation in pipes [3] and technical applications in fields such as structure-borne sound analysis and power ultrasonics.

The simplest mathematical approach to the problem consists in using elementary rod theory in conjunction with idealized transition conditions at the discontinuity. This approach leads to an exceptionally simple boundary-value problem lending itself to analysis but, in exchange, its validity is known to be restricted to slender rods, low frequencies [2, 4, 5] and modest cross-section jumps.

The validity ranges can be extended by introducing improved rod theories [4] and considering ways of more realistic modelling of transition conditions [6]. But before proceeding to more complex mathematical models it would be appropriate to extract as much information as possible from the simplest one. This, in the author's opinion, is the *raison d'être* of simple models and constitutes the purpose of the present letter.

Thus, we consider the free longitudinal vibrations of the rod shown in Figure 1 for which the simple eigenanalysis leads to the following commonplace results for different sets of simple boundary conditions.

*Fixed-free rod.* Eigenequation [1]:

$$\cos \beta + (\gamma - 1) \cos \alpha \beta \cos(1 - \alpha)\beta = 0. \quad (1)$$

*r*th eigenfunction:

$$U_r(\xi) = \begin{cases} \sin \beta_r \xi, & 0 \leq \xi \leq \alpha, \\ A_r \sin(\beta_r \xi - \varphi_r), & \alpha \leq \xi \leq 1, \end{cases} \quad (2)$$

where

$$A_r = \sqrt{1 + (\gamma^2 - 1) \cos^2 \alpha \beta_r}, \quad \varphi_r = \arctan \left[ \frac{(\gamma - 1) \sin \alpha \beta_r \cos \alpha \beta_r}{1 + (\gamma - 1) \cos^2 \alpha \beta_r} \right]. \quad (3)$$

*Fixed-fixed rod.* Eigenequation:

$$\sin \beta + (\gamma - 1) \cos \alpha \beta \sin(1 - \alpha)\beta = 0, \quad (4)$$

*r*th eigenfunction is as already given in equations (2) and (3).

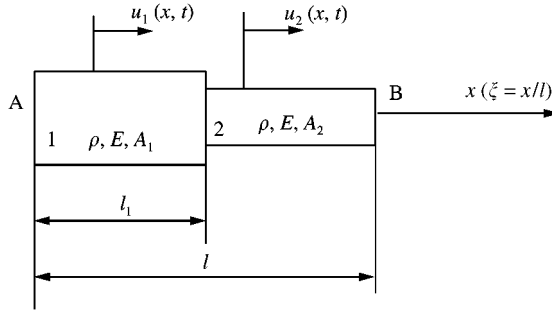


Figure 1. Rod with a cross-section discontinuity.

*Free-free rod.* Eigenequation [2]:

$$\sin \beta + (\gamma - 1) \sin \alpha \beta \cos(1 - \alpha)\beta = 0. \quad (5)$$

*r*th eigenfunction:

$$U_r(\xi) = \begin{cases} \cos \beta_r \xi, & 0 \leq \xi \leq \alpha, \\ A_r \cos(\beta_r \xi - \varphi_r), & \alpha \leq \xi \leq 1, \end{cases} \quad (6)$$

where

$$A_r = \sqrt{1 + (\gamma^2 - 1) \sin^2 \alpha \beta_r}, \quad \varphi_r = \arctan \left[ \frac{(1 - \gamma) \sin \alpha \beta_r \cos \alpha \beta_r}{1 - (1 - \gamma) \sin^2 \alpha \beta_r} \right]. \quad (7)$$

In equations (1-7)  $\beta = \sqrt{(\rho \ell^2 / E)} \omega$ , where  $\omega$  is the eigenfrequency,  $\xi = x/\ell$ ,  $\alpha = \ell_1/\ell$ ,  $\gamma = A_1/A_2$  (cross-section ratio),  $\beta_r$  is the *r*th root of equation (1), (4) or (5) depending on the context,  $\rho$ ,  $E$  and  $\ell$  are the mass density, Young's modulus of elasticity and total length of the rod, respectively, and the amplitude of the first portion of  $U_r(\xi)$  in equations (3) and (6) is arbitrarily taken as unity.

In section 2 of this letter we elaborate on the immediate results given above and deduce further closed-form information on the behaviour of the eigencharacteristics. This, in turn, makes it possible for *ad hoc* approximate formulae to be given for the infinite sequence of eigencharacteristics, as is done in section 3. Finally, section 4 points out certain isospectrality relations between the analyzed rods.

## 2. ELABORATED RESULTS

### 2.1. FIXED-FREE ROD

For further reference note first that when  $\gamma = 1$ ,  $\alpha = 0$  or 1 both eigenequation (1) and *r*th eigenfunction (2) reduce, as they should, to those of a uniform fixed-free rod, namely  $\cos \beta = 0$  whose roots are

$$\beta_r^0 = (2r - 1) \frac{\pi}{2}, \quad r = 1, 2, \dots \quad (8)$$

and  $U_r^0(\xi) = C_r \sin \beta_r^0 \xi$  ( $C_r$ : arbitrary constant), whose nodes (fixed end included) and antinodes (free end included) are situated, respectively, at

$$\xi_{r,n}^N = \frac{(2n-2)}{(2r-1)}, \quad \xi_{r,n}^{AN} = \frac{(2n-1)}{(2r-1)}, \quad n = 1, 2, \dots, r. \quad (9)$$

Inserting the  $\beta_r^0$  values of equation (8) into equation (1) and solving the latter for  $\alpha$ , one finds out that there are two sets of cross-section change location  $\alpha$  for which the  $r$ th eigenfrequency of the uniform rod is preserved. These are nothing but the nodes and antinodes given in equation (9). As a matter of fact one observes in Figure 2(a), where the first four roots  $\beta_r$  of equation (1) are plotted versus  $\alpha$  for four different values of  $\gamma$ , that each  $\beta_r$  line oscillates about the corresponding  $\beta_r^0$  line (labelled  $\gamma = 1$ ) intersecting it at the nodes and antinodes of the  $r$ th mode. In between, there are certain  $\alpha$  points where maximal departure of  $\beta_r$  from  $\beta_r^0$  occurs. It is possible to get information about these points by calculating  $d\beta/d\alpha$  and  $d^2\beta/d\alpha^2$  from equation (1) by using differentiation rules of implicit functions and following the usual procedures of the classical min-max theory. After some calculation one finds out that the extrema lie on members with parameter values  $s = 0, \mp 1, \mp 2, \dots$  of the parametric family of curves

$$\alpha(s, \beta) = \frac{1}{2} + \frac{s\pi}{2\beta} \quad (10)$$

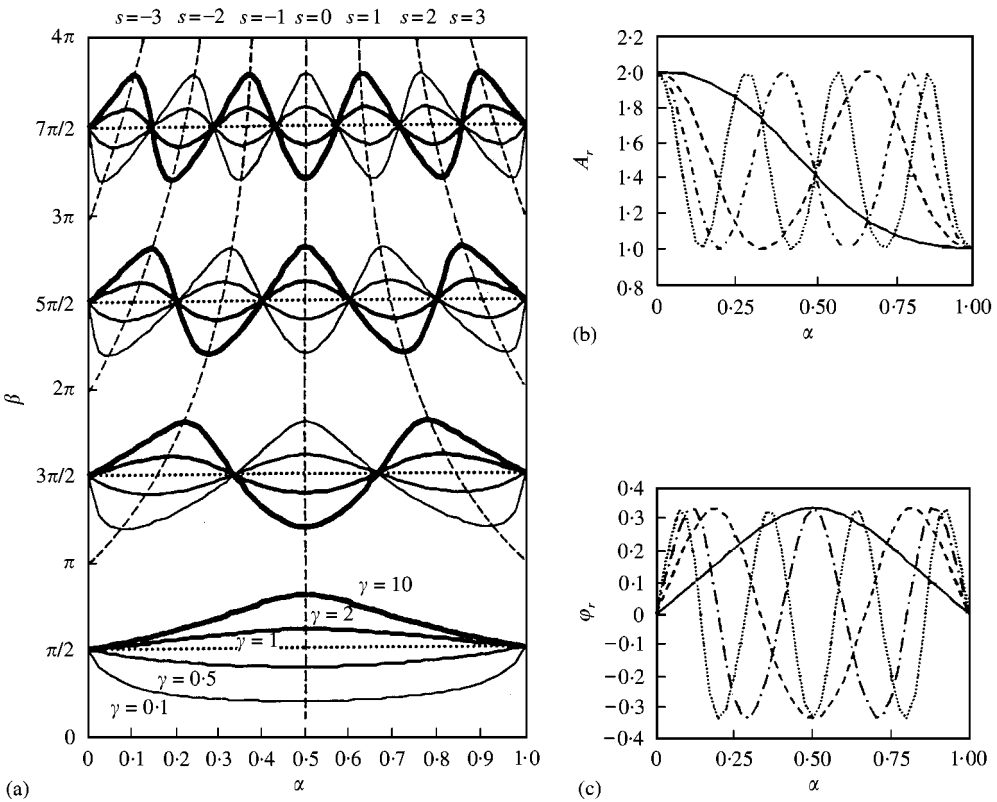


Figure 2. Fixed-free rod. Dependence of the eigenparameters on the cross-section change location: (a) eigenfrequencies, (b) amplitude ratio, (c) phase shift between the two portions of the eigenfunctions for  $\gamma = 2, \dots$ ,  $r = 1$ ;  $-$ ,  $r = 2$ ;  $- \cdot -$ ,  $r = 3$ ;  $\cdots \cdots$ ,  $r = 4$ .

(see Figure 2(a)), that the minimal and maximal values of  $\beta_r$  are

$$\beta_{r,\min,\max} = \beta_r^0 \mp \Delta\beta, \quad r = 1, 2, \dots, \quad (11)$$

where

$$\Delta\beta = \arcsin\left(\frac{|1 - \gamma|}{1 + \gamma}\right) \quad (12)$$

irrespective of mode number  $r$ , and that maxima occur at the points

$$\alpha_{r,s}^M = \frac{1}{2} + \frac{1}{2} \frac{s\pi}{[r\pi - \arccos(|1 - \gamma|/(1 + \gamma))]}, \quad s = \mp \ell_M, \quad \mp(\ell_M + 2), \dots, \quad \mp(u_M - 2), \quad \mp u_M, \quad (13)$$

$$\ell_M = \frac{[1 - (-1)^r \operatorname{sgn}(1 - \gamma)]}{2}, \quad u_M = r - \frac{[3 + 1 \operatorname{sgn}(1 - \gamma)]}{2};$$

while minima occur at

$$\alpha_{r,s}^m = \frac{1}{2} + \frac{1}{2} \frac{s\pi}{[(r-1)\pi + \arccos(|1 - \gamma|/(1 + \gamma))]}, \quad s = \mp \ell_m, \quad \mp(\ell_m + 2), \dots, \quad \mp(u_m - 2), \quad \mp u_m, \quad (14)$$

$$\ell_m = \frac{1 + (-1)^r \operatorname{sgn}(1 - \gamma)}{2}, \quad u_m = r - \frac{[3 - 1 \operatorname{sgn}(1 - \gamma)]}{2};$$

Equation (12) shows that  $\Delta\beta$  reduces to zero when  $\gamma = 1$  and tends to  $\pi/2$  in the extremal cases where  $\gamma$  tends to zero or infinity. Thus, one concludes that  $\pi/2$  constitutes an upper limit for the eigenvalue shifting caused by a cross-section discontinuity.

Turning now ones attention to the eigenfunctions and considering first  $A_r$  of equation (3) which defines the amplitude ratio of the second to the first portion of the  $r$ th eigenfunction one notes that when  $\alpha$  changes this ratio will change between the extremal values of  $\gamma$  and 1, irrespective of mode number  $r$ . As can be checked by direct substitution of  $\zeta_{r,n}^N$  and then of  $\zeta_{r,n}^{AN}$  for  $\alpha$ , and consequently  $\beta_r^0$  for  $\beta_r$  from equations (9) and (8) into equations (2) and (3), these extremal values occur when the cross-section change is placed at a node or an antinode of the uniform beam respectively. These features can be seen in Figure 2(b), where the first four  $A_r$  values are plotted versus  $\alpha$  for  $\gamma = 2$ . Inspection of this figure also shows that the value of  $A_r$  is independent of  $r$  when  $\alpha = 0.5$ . This value can be calculated from equations (1) and (3) to be  $A = \sqrt{\gamma}$ .

Next consider  $\varphi_r$  of equation (3) which defines the phase shift between the two portions of the  $r$ th eigenfunction, i.e., controls the distance between two successive nodes (and antinodes) intercepting the discontinuity. Substitutions similar to those above from equations (8) and (9) into equations (2) and (3) show that  $\varphi_r$  reduces to zero when the cross-section discontinuity is placed at a node or an antinode of the  $r$ th mode of the uniform rod. On the other hand, the extremal values  $\varphi_r$  may take on, can be calculated from equation (3), by applying the necessary conditions for an extremum, to be

$$\varphi_{r,\min,\max} = \mp \arctan\left(\frac{|1 - \gamma|}{2\sqrt{\gamma}}\right) \quad (15)$$

irrespective of mode number  $r$ . These results are visible in Figure 2(c) where the first four  $\varphi_r$  values are plotted versus  $\alpha$  for  $\gamma = 2$ . Equation (15) shows that the extremal values of  $\varphi_r$  tend to  $\pm \pi/2$  in the extremal cases, where  $\gamma$  tends to zero or infinity and therefore that its absolute value is always less than  $\pi/2$ .

2.2. FIXED-FIXED ROD

When either  $\gamma = 1, \alpha = 0$  or  $\alpha = 1$ , eigenequation (4) and eigenfunction (2) reduce to those of a uniform fixed-fixed rod, namely  $\sin \beta = 0$  and  $U_r^0(\xi) = C_r \sin \beta_r^0 \xi$ . For further reference we note that the roots of the former are

$$\beta_r^0 = r\pi, \quad r = 1, 2, \dots \tag{16}$$

and the nodes (fixed ends included) and antinodes of the latter are situated at

$$\xi_{r,n}^N = \frac{(n-1)}{r}, \quad n = 1, 2, \dots, r+1, \quad \xi_{r,n}^{AN} = \frac{(2n-1)}{2r}, \quad n = 1, 2, \dots, r. \tag{17}$$

An analysis shows that most of the results of section 2.1 do also hold for the present case. As the results common to all the three considered boundary conditions will be summarized in section 2.4, only results which are peculiar to rods with fixed-fixed boundary conditions will be given here. Figure 3(a) shows the first four roots  $\beta_r$  of equation (4) plotted versus  $\alpha$  for four different  $\gamma$  values. The extrema of  $\beta_r$ 's can now be shown to be situated on curves  $s = 1, 2, \dots$  of the parametric families

$$\alpha(s, \beta) = \frac{1}{2} \mp \frac{(2s-1)\pi}{4\beta} \tag{18}$$

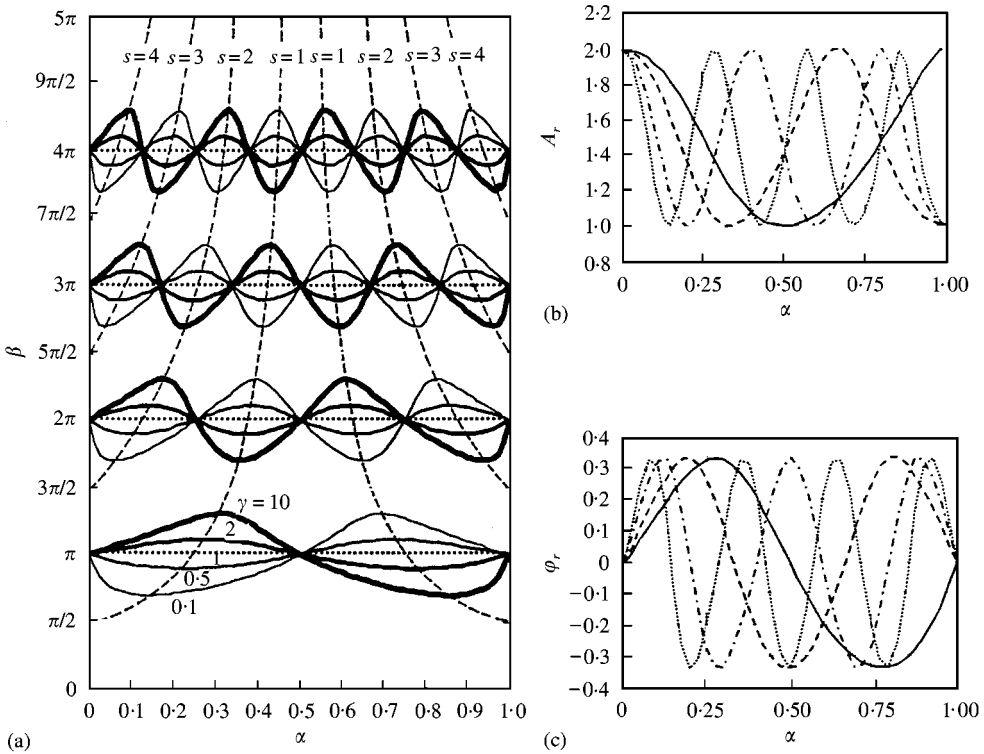


Figure 3. Fixed-fixed rod. Dependence of the eigenparameters on the cross-section change location: (a) eigenfrequencies, (b) amplitude ratio, (c) phase shift between the two portions of the eigenfunctions for  $\gamma = 2$ , —,  $r = 1$ ; - - -,  $r = 2$ ; - · - ·,  $r = 3$ ; · · · · ·,  $r = 4$ .

their values being as given in equation (11), where  $\beta_r^0$  must be substituted from equation (16) and again

$$\Delta\beta = \arcsin\left(\frac{|1-\gamma|}{1+\gamma}\right) \quad (19)$$

for any mode. Maxima occur when the cross-section change is placed at the points

$$\alpha_{r,s}^M = \frac{1}{2} + \operatorname{sgn}(1-\gamma) \frac{(-1)^{r-s}}{4} \frac{(2s-1)\pi}{[r\pi + \arcsin(|1-\gamma|/(1+\gamma))]}, \quad s = 1, 2, \dots, r, \quad (20)$$

while minima occur at

$$\alpha_{r,s}^m = \frac{1}{2} - \operatorname{sgn}(1-\gamma) \frac{(-1)^{r-s}}{4} \frac{(2s-1)\pi}{[r\pi - \arcsin(|1-\gamma|/(1+\gamma))]}, \quad s = 1, 2, \dots, r. \quad (21)$$

Figure 3(b) and 3(c) shows the first four  $A_r$  and  $\varphi_r$  values plotted on  $\alpha$  for  $\gamma = 2$ .

### 2.3. FREE-FREE ROD

We again note that when either  $\gamma = 1$ ,  $\alpha = 0$  or  $\alpha = 1$  both eigenequation (5) and eigenfunction (6) reduce to those of a uniform free-free rod, namely  $\sin \beta = 0$ , whose roots are

$$\beta_r^0 = r\pi, \quad r = 0, 1, 2, \dots \quad (22)$$

and  $U_r^0(\xi) = C_r \cos \beta_r^0 \xi$  whose nodes and antinodes (free ends included) are situated at

$$\xi_{r,n}^N = \frac{(2n-1)}{2r}, \quad n = 1, 2, \dots, r, \quad \xi_{r,n}^{AN} = \frac{(n-1)}{r}, \quad n = 1, 2, \dots, r+1. \quad (23)$$

The first four roots  $\beta_r$  of equation (5) ( $\beta_0 = 0$  of the rigid-body mode excluded) are plotted versus  $\alpha$  for four different  $\gamma$  values in Figure 4(a). The loci of the extrema of various  $\beta_r$  lines and their extremal values can be shown to coincide with those given in equations (11), (18) and (19). However, the locations of the maxima and minima are now

$$\alpha_{r,s}^M = \frac{1}{2} - \operatorname{sgn}(1-\gamma) \frac{(-1)^{r-s}}{4} \frac{(2s-1)\pi}{[r\pi + \arcsin(|1-\gamma|/(1+\gamma))]}, \quad s = 1, 2, \dots, r, \quad (24)$$

$$\alpha_{r,s}^m = \frac{1}{2} + \operatorname{sgn}(1-\gamma) \frac{(-1)^{r-s}}{4} \frac{(2s-1)\pi}{[r\pi - \arcsin(|1-\gamma|/(1+\gamma))]}, \quad s = 1, 2, \dots, r. \quad (25)$$

Finally, the first four  $A_r$  and  $\varphi_r$  values are plotted on  $\alpha$  for  $\gamma = 2$  in Figure 4(b) and 4(c).

### 2.4. GENERALIZATIONS

Conclusions which are common to all the three boundary conditions considered above may be summarized as follows: (1) Placing a cross-section change at an antinode of the  $r$ th mode of the uniform rod is of no consequence on either of its  $r$ th eigencharacteristics. (2) Placing a cross-section change at a node of the  $r$ th mode of the uniform rod does not alter the  $r$ th eigenfrequency or the positions of the nodes and antinodes of the  $r$ th mode but alters the  $r$ th mode shape so that the amplitude of the second portion is  $\gamma$  times that of the first. (3) Placing a cross-section change at a point which is neither a node nor an antinode of the uniform rod's  $r$ th mode influences all its  $r$ th eigencharacteristics. The maximal value of

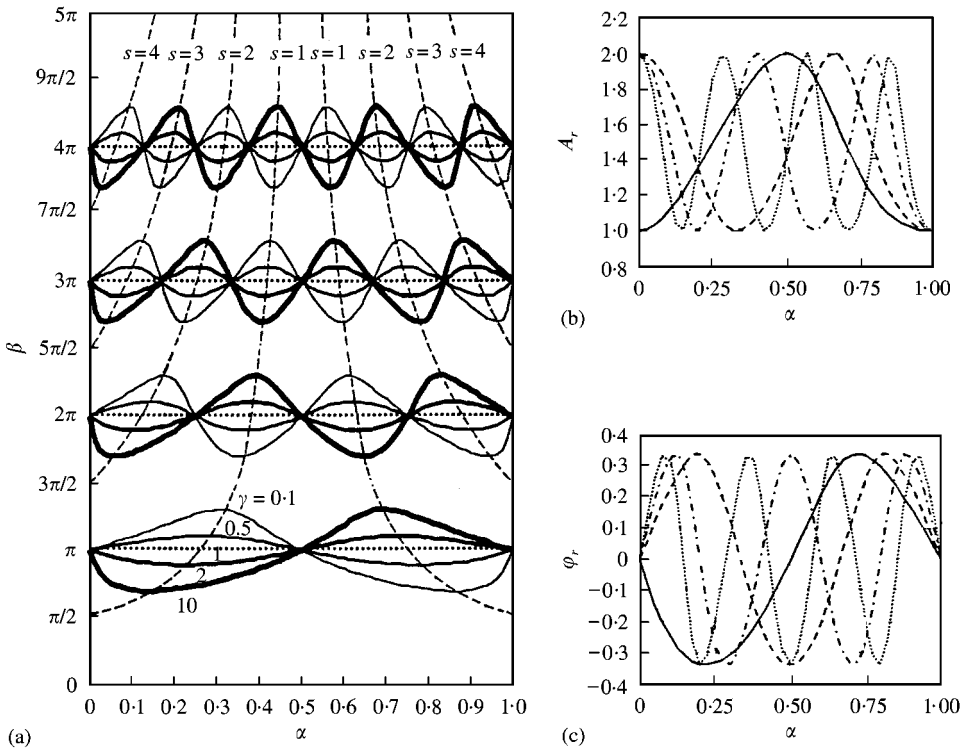


Figure 4. Free-free rod. Dependence of the eigenparameters on the cross-section change location: (a) eigenfrequencies, (b) amplitude ratio, (c) phase shift between the two portions of the eigenfunctions for  $\gamma = 2$ : —,  $r = 1$ ; - -,  $r = 2$ ; - · -,  $r = 3$ ; -----,  $r = 4$ .

the resulting shift of an eigenvalue  $\beta_r^0$  is as given in equation (12), thus, always less than  $\pi/2$ , the amplitude ratio  $A_r$  of the second to the first portion of the  $r$ th eigenfunction between 1 and  $\gamma$  (Figures 2(b), 3(b), 4(b)) and the extremal values of the phase shift  $\phi_r$  between the two portions of the  $r$ th eigenfunction are as given in equation (15) (Figures 2(c), 3(c), 4(c)), thus always less than  $\pi/2$  in absolute value.

### 3. AN APPROXIMATE EIGENANALYSIS

It should be observed that Figures 2(a), 3(a) and 4(a) have a very orderly structure. In view of the fact that the problem of determining the rules governing the order of these figures and that of finding closed-form general solutions to the related eigenequation are two aspects of the same mathematical problem one is led to have a closer look at the apparently simple order of these figures and try to extract its internal logic. It should, however, be clear that as no exact solution in terms of known functions can be given for the corresponding eigenequations, no exact rule can be expected to be determined of the order of these figures how simple it may look. We will, therefore try here humbly, to guess these rules approximately and thereby propose approximate closed-form formulae for the eigencharacteristics in terms of known functions. Reconsidering the figures with this goal in mind, one notices that the  $\beta_r(\alpha)$  lines can reasonably be assumed to evolve from ordinary sine curves

$$\bar{\beta}_r = \beta_r^0 \pm \Delta\beta \sin\left(\frac{2\pi\alpha}{\lambda_r}\right) \quad (26)$$

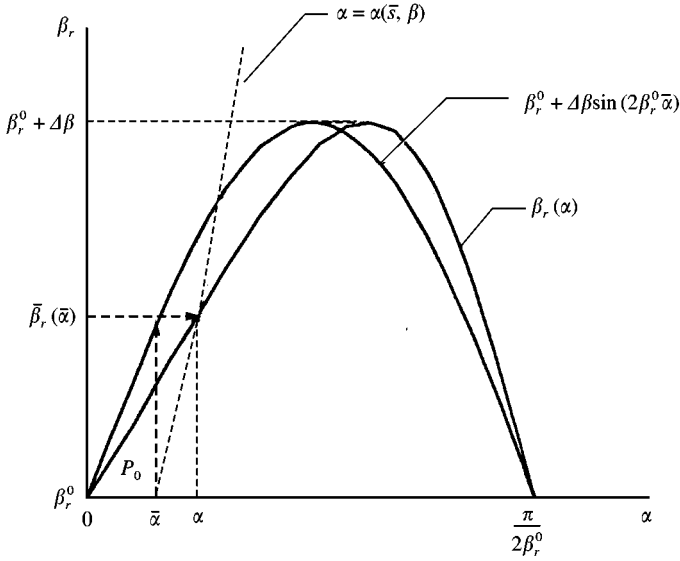


Figure 5. Assumed construction of  $\beta_r(\alpha)$  curves.

through a mapping which horizontally projects the points of vertical lines  $\alpha = \bar{\alpha}$  onto the parametric curve  $\alpha = \alpha(s, \beta)$  passing through the point  $P_0(\bar{\alpha}, \beta_r^0)$  (Figure 5). Note that this assumption holds good at  $\alpha$  values corresponding to nodes and antinodes of the uniform rod and those where extrema of  $\beta_r$  occur. As the equations of the parametric curves  $\alpha = \alpha(s, \beta)$  as well as the amplitudes  $\Delta\beta$  and the wavelengths

$$\lambda_r = 2 |\zeta_{r,n}^{AN} - \zeta_{r,n}^N| = \frac{\pi}{\beta_r^0} \tag{27}$$

of the hypothetical sine curves are known from the content of section 2, approximate formulae can easily be given on the basis of the above assumption for the eigenvalues  $\beta_r$ , and this will be done in what follows.

### 3.1. FIXED-FREE ROD

For a fixed-free rod, using equations (8), (9), (12) and (27), equation (26) may be written as

$$\bar{\beta}_r(\bar{\alpha}) = \beta_r^0 - \text{sgn}(1 - \gamma) \Delta\beta \sin(2\beta_r^0 \bar{\alpha}), \quad r = 1, 2, \dots \tag{28}$$

Inserting the co-ordinates  $\bar{\alpha}$  and  $\beta_r^0$  of the point  $P_0$  into equation (10) and solving for  $s$  one finds out that the required parametric curve corresponds to the parameter value  $\bar{s} = (2\bar{\alpha} - 1) \beta_r^0 / \pi$ . Substituting this and equation (28) into equation (10) and solving for  $\alpha$  one obtains

$$\alpha(\bar{\alpha}) = \frac{1}{2} + \left( \bar{\alpha} - \frac{1}{2} \right) \frac{\beta_r^0}{\bar{\beta}_r(\bar{\alpha})}, \tag{29}$$

where  $\bar{\beta}_r(\bar{\alpha})$  is to be substituted from equation (28). Equations (28) and (29) constitute a parametric representation, with  $\bar{\alpha}$  as the parameter, of the proposed approximation for the



$\beta_r(\alpha)$  curves. For any given  $\bar{\alpha}$  value, the  $r$ th eigenvalue corresponding to the  $\alpha$  value given by equation (29) can be calculated approximately from equation (28). It would of course be desirable to obtain a closed-form formula for  $\beta_r(\alpha)$  rather than a parametric representation. To this end expand the right-hand side of equation (29) into a Taylor series about  $\alpha$ , retain only linear terms and solve for  $\bar{\alpha}$  to obtain

$$\bar{\alpha}(\alpha) \cong \alpha + \frac{1}{2} \frac{\bar{\beta}_r(\alpha)/\beta_r^0 - 1}{[1/(2\alpha - 1) + \text{sgn}(1 - \gamma)\Delta\beta(\bar{\beta}_r^0/\bar{\beta}_r(\alpha)) \cos(2\beta_r^0\alpha)]}, \quad (30)$$

where  $\bar{\beta}_r(\alpha)$  is to be substituted from equation (28) with  $\alpha$  as the argument. Now, the  $r$ th eigenvalue  $\beta_r$  can approximately be calculated from equations (28) and (30) for any given  $\alpha$  and  $\gamma$  values. Also, an approximation for the  $r$ th eigenfunction can be obtained by substituting the approximate value of  $\beta_r$  into equations (2) and (3). To give an idea about the performance of the approximate formula, the percentage error committed in the calculation of  $\beta_1$  through equations (28) and (30) is plotted versus  $\alpha$  for  $\gamma = \frac{1}{2}, \frac{3}{4}, \frac{4}{3}$  and 2 in Figure 6(a). Higher eigenvalues are not considered here because the largest error percentage occurs in the calculation of  $\beta_1$ . Upon inspection of Figure 6(a) one observes that the error remains at the order of 0.01% for  $\gamma$  values close to 1 such as  $\gamma = 3/4$  and  $4/3$ , that it quickly grows larger with  $\gamma$  getting away from 1, but that it still does not exceed 0.1% for  $\gamma = 2$  and 0.35% for  $\gamma = 1/2$ . The performance of the approximate formula is therefore satisfactory for many practical purposes with the restriction that it is not used for  $\gamma$  values too far from unity.

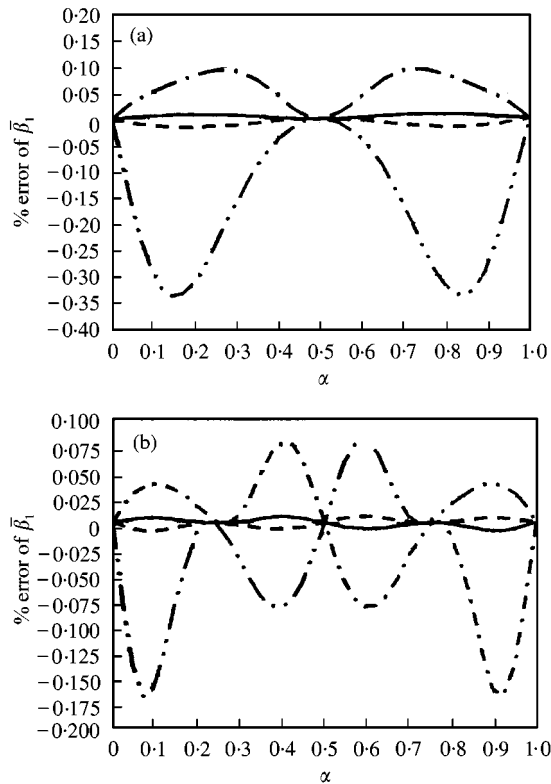


Figure 6. Accuracy of the approximation: (a) fixed-free, (b) fixed-fixed rod (---,  $\gamma = 2$ ; —,  $\gamma = 4/3$ ; - - ,  $\gamma = 3/4$ ; ····,  $\gamma = 1/2$ ).

However, ultimately, this should not be considered as a true restriction because the uniform stress distribution assumption implicit in the elementary rod theory and the idealized transition conditions used here, already restricts the validity of the present analysis to  $\gamma$  values close to unity.

### 3.2. FIXED-FIXED AND FREE-FREE RODS

Repeating the above analysis for fixed-fixed rods by using equations (16–19), (26) and (27) one obtains exactly the same results as given in equations (28–30). However, now  $\beta_r^0$  and  $\Delta\beta$  are, of course, those given in equations (16) and (19) respectively.

Finally, repeating once again the analysis for the vibrating modes of free-free rods by using equations (18), (19), (22), (23), (26) and (27) the results are again similar to those presented in equations (28–30). The only difference is that the argument of the signum function in equations (28) and (30) must now read as  $(\gamma - 1)$  instead of  $(1 - \gamma)$ . It should be clear that now  $\beta_r^0$  and  $\Delta\beta$  are those given in equations (22) and (19) respectively.

The percentage error of a fundamental frequency calculation for fixed-fixed rods using equations (28) and (30) is plotted on  $\alpha$  for various  $\gamma$  values in Figure 6(b). The same figure can also be used for free-free rods by substituting  $1/\gamma$  for  $\gamma$  or  $1 - \alpha$  for  $\alpha$ . This figure shows that the accuracy of the approximate formula is also satisfactory for fixed-fixed and free-free rods, subject to the restriction voiced above.

### 4. SOME REMARKS ON ISOSPECTRAL RODS

Two vibratory systems having the same frequency spectrum (or identical eigenequations) are said to be isospectral [7]. The existence of isospectral fixed-free rods was pointed out in reference [8] and the general problem of obtaining rods which are isospectral to a given one was treated in reference [7]. Our aim here is to underline certain isospectrality relations between stepped rods as deduced from the foregoing analysis.

First, consider fixed-free rods and note that eigenequation (1) is invariant under permutation of  $\alpha$  and  $(1 - \alpha)$  (or that Figure 2(a) is symmetrical with respect to the line  $\alpha = 0.5$ ). The conclusion is that two fixed-free rods with similar cross-section ratio  $\gamma$  and with the lengths of the two portions interchanged are isospectral to each other. This actually constitutes a discontinuous example to a rule well established for rods with continuous cross-section change, namely two fixed-free rods with cross-sections  $A_1(\xi)$  and  $A_2(\xi) = C/A_1(1 - \xi)$  are isospectral [7, 8].

Next, consider fixed-fixed and free-free rods and note that substitution of either  $1/\gamma$  for  $\gamma$  or  $(1 - \alpha)$  for  $\alpha$  into equation (4) yields equation (5) and *vice versa*. As a result of this, Figures 3(a) and 4(a) can be obtained from one another by relabelling the lines  $\gamma$  as  $1/\gamma$  or by inverting the figure with respect to the line  $\alpha = 0.5$ . The conclusion is that a stepped free-free rod is isospectral (with the zero eigenvalue corresponding to the rigid-body mode excluded) to a fixed-fixed one obtained by interchanging the lengths of the two portions or (which is the same thing) inverting the cross-section ratio. Again a discontinuous example to the general rule [7] establishing that a free-free rod with continuous cross-section  $A_1(\xi)$  is isospectral to a fixed-fixed rod with cross-section  $A_2(\xi) = C/A_1(\xi)$  is in question.

Finally, noting that for  $\alpha = 0.5$  both eigenequations (4) and (5) reduce to the eigenequation common to the uniform fixed-fixed and free-free rods (or that all the  $\beta_r$  lines of Figures 3(a) and 4(a) intersect the  $\beta_r^0$  line at  $\alpha = 0.5$ ), one concludes that all fixed-fixed and free-free rods with a cross-section change at their midpoint are isospectral

(zero eigenvalue of free-free rods excluded) whatever their cross-section ratio  $\gamma$  may be (also  $\gamma = 1$ ).

## 5. CONCLUSIONS

The effect of a cross-section discontinuity on the eigencharacteristics of longitudinally vibrating rods is studied. Certain general features of the dependence of the eigenvalues and eigenfunctions on the position and magnitude of the cross-section change are determined and closed-form formulae are proposed which approximately describe this functional dependence.

Although the interest is focused on the longitudinal vibrations of rods in this study, it should be noted that due to the mathematical equivalence and physical conjugacy of the problems, all the results are equally applicable to the torsional vibrations of bars and wave propagation in pipes with cross-section discontinuities by appropriate redefinition of the parameters  $\beta$  and  $\gamma$ .

## REFERENCES

1. J. L. HUMAR 1990 *Dynamics of Structures*. Englewood Cliffs, NJ: Prentice-Hall.
2. K. F. GRAFF 1975 *Wave Motion In Elastic Solids*. New York: Dover.
3. L. E. KINSLER *et al.* 1982 *Fundamentals of Acoustics*. New York: Wiley; third edition.
4. J. S. RAO 1992 *Advanced Theory of Vibration*. New York: Wiley.
5. J. W. S. RAYLEIGH 1945 *The Theory of Sound*, New York: Dover; second edition.
6. W. SEEMANN 1996 *Journal of Sound and Vibration* **198**, 571–587. Transmission and reflection coefficients for longitudinal waves obtained by a combination of refined rod theory and FEM.
7. G. M. L. GLADWELL and A. MORASSI 1995 *Inverse Problems* **11**, 533–554. On isospectral rods, horns and strings.
8. Y. M. RAM and S. ELHAY 1995 *Journal of Sound and Vibration* **184**, 759–766. Dualities in vibrating rods and beams: continuous and discrete models.